

Surface structures and thermal vibrations of Ni and Cu thin films studied by extended x-ray-absorption fine structure

Manabu Kiguchi, Toshihiko Yokoyama, Daiju Matsumura, Hiroshi Kondoh, Osamu Endo, and Toshiaki Ohta
Department of Chemistry, Graduate School of Science, The University of Tokyo, 7-3-1 Hongo, Bunkyo-ku, Tokyo 113-0033, Japan
(Received 14 October 1999; revised manuscript received 18 January 2000)

Temperature- and angle-dependent extended x-ray-absorption fine-structure spectra of Cu and Ni thin films grown epitaxially on highly oriented pyrolytic graphite were measured and analyzed in order to investigate the dynamical properties of the surface metal-metal bonds. From the mean-square relative displacements of the metal-metal bonds, the effective Debye temperatures of the surface in-plane and out-of-plane bonds were determined. The surface bonds were found to be much softer and anharmonic, especially for the surface normal direction, than those of the corresponding bulk metals. We have also carried out classical Monte Carlo simulations for Cu films based on the embedded-atom method. The experimental results were reproduced qualitatively well and it was clarified that the out-of-plane bonds between the first and the second layer are noticeably weaker than the other bonds such as the in-plane bond in the first layer.

I. INTRODUCTION

Enhancement of anharmonic vibration of surface atoms has been an attractive subject since it is believed to be a trigger of surface melting and consequent bulk melting. Anharmonicity is especially important because no melting should occur within harmonic interatomic potentials. In order to investigate a huge enhancement of anharmonic vibration and surface melting, several sophisticated techniques such as low-energy electron diffraction¹⁻⁴ (LEED) and ion scattering^{5,6} have been applied. The LEED study¹ revealed that on Ni(100) the surface thermal expansion coefficient rapidly increases between 900 and 1300 K, reaching a value nearly 20 times larger than that in the bulk. The ion-scattering works⁶ clarified that the open (110) faces of fcc metals like Pb and Al exhibit surface melting; the surface melting point of Pb(110) is approximately 40 K lower than bulk melting point.

Although most of these works have paid attention to long-range order, local structure is also very important since melting occurs through short-range atomic mechanisms.⁷ The extended x-ray-absorption fine-structure (EXAFS) technique is one of the most suitable methods to investigate the dynamical properties of the surface bonds since it provides local information on thermal disorder including anharmonicity. Moreover, polarization-dependent measurements allow one to study vibrational anisotropy. It is, however, rather difficult to record surface EXAFS spectra of metal single crystals because of the presence of huge contribution from bulks. Therefore, except for adsorbate-substrate systems, most previous EXAFS works on surface vibrational properties were devoted to small metal clusters.⁸⁻¹¹ By changing the particle size, the thermal vibration and anharmonicity of surface bonds in small metal clusters were actually found to be enhanced significantly. The other techniques such as x-ray diffraction¹² and TEM (transmission electron microscope)¹³ were also used for studying thermal properties of small metal clusters. The TEM experiments clarified the decrease in melting temperature for Au clusters.¹³

Since information on vibrational anisotropy cannot directly be obtained from small clusters, studies concerning single crystals are still essential to distinguish the out-of-plane bonds from the in-plane ones. The LEED experiments¹⁻⁴ have clarified significant anisotropy between surface normal and parallel directions. On the other hand, Roubin *et al.*¹⁴ have measured surface EXAFS of monolayer Co deposited on Cu(111) to eliminate the bulk contribution to the surface EXAFS spectra by changing the adsorbate element from the substrate. They have concluded that the out-of-plane Co-Cu bond is again noticeably softer than the in-plane Co-Co one.

In the present study, we have investigated vibrational anisotropy of ultrathin films grown epitaxially on a certain substrate by means of the temperature- and angle-dependent EXAFS technique. The ultrathin films allows us to obtain local information on surface metal-metal bonds without taking care of inequivalent bond natures as in the case of Co/Cu(111). There have been reported several epitaxial metal films; Ag deposited on Si(111) and HOPG (highly oriented pyrolytic graphite) is known to form flat (111)-oriented islands.¹⁵⁻¹⁷ In the case of Ni/HOPG, Bäumer *et al.*¹⁸ have reported that the (111)-oriented islands are formed at low temperature. Marcus and Hinnen¹⁹ have also found for the Cu/HOPG system that even at room temperature Cu films grow on HOPG in a layer-by-layer fashion. In this paper, we have thus chosen Cu and Ni ultrathin epitaxial films on HOPG. For further understanding of surface vibrational properties, we have also carried out classical Monte Carlo (MC) simulations for Cu films using the embedded-atom method (EAM).

II. EXPERIMENT

A HOPG (ZYA grade) substrate was cleaved with Scotch tape in air and mounted in an ultrahigh vacuum chamber. The HOPG was annealed at 1200 K for 1 min to remove contaminations at the surface.^{18,19} After cooling down to 120 K, Ni or Cu was deposited on the clean HOPG. The film thickness and growth rate were monitored by a quartz crystal

oscillator placed near the sample. The absolute and precise thickness was determined by inductivity-coupled plasma emission spectroscopy after all the EXAFS measurements. Although the growth style of Ni or Cu could not be characterized in the present chamber for the EXAFS measurements, LEED observation was carried out in advance using a different chamber employing the same deposition condition. We verified beautiful sixfold spots, which implies the growth of (111) oriented epitaxial films.

Ni and Cu *K*-edge XAFS (x-ray-absorption fine-structure) measurements were carried out at the hard x-ray double-crystal monochromator stations BL7C and BL12C of Photon Factory in the Institute of Materials Structure Science.²⁰ The fluorescence yield detection method was employed to obtain Ni and Cu *K*-edge XAFS using a SSD (solid-state detector). For the normalization of the fluorescence yield spectra, the intensity of the incident x rays was measured with an ionization chamber filled with pure N₂ as a detection gas. The XAFS spectra were taken at normal ($\theta=90^\circ$) and grazing ($\theta=30^\circ$) x-ray incident angles. At normal x-ray incidence, the electric field vector \mathbf{E} of the x rays lies parallel to the surface plane and mainly the in-plane bonds contribute to EXAFS, while at grazing x-ray incidence, \mathbf{E} lies close to surface normal, implying that the dominant contribution is of the out-of-plane bonds. The measurements were done at 120, 300, and 420 K. For the measurements at 120 K, the sample crystal was cooled down using a liquid-N₂ cryostat. The sample temperature was monitored with a Chromel-Alumel thermocouple, which was spot-welded on a Ta sheet attached to the sample surface. The temperature fluctuations were less than ± 3 K during the XAFS measurements.

III. EXPERIMENTAL RESULTS

A. Characterization of Cu thin films

First, we have characterized the structures of the Cu films by LEED. The HOPG misses common orientation with respect to the crystallographic directions within the plane. Thus, the Debye-Scherrer rings were observed instead of spots. After deposition of Cu at 120 K and subsequent annealing to 300 K, clear hexagonal spots appeared. This indicates that (111)-oriented Cu islands were formed on the HOPG as in the previous case of Ag/Si(111).¹⁷ After deposition at low temperature, the film is considered to consist of an assembly of small crystals with a majority of (111)-faced crystals. Such an initial stage may be converted into large crystals (epitaxial film) after annealing.

15 ML Cu was deposited at 120 K, and subsequently annealed to 300 and 420 K. In each step, the XAFS spectrum was measured. Figure 1 shows the change of Cu *K*-edge XANES (x-ray-absorption near-edge structure) spectra. For comparison, the spectrum of a Cu foil was also displayed in Fig. 1. For bulk fcc Cu, two characteristic peaks appear after the absorption edge. Theoretical calculations revealed that they correspond to fourth and higher shell atoms.⁹ The absence of the two peaks in the 120-K spectrum indicates that this film does not crystallize so well. After annealing to 300 and 420 K, the characteristic peaks appear, implying the growth of well-defined films.

We will subsequently discuss the crystal growth in terms of structure by using EXAFS. Extraction of the EXAFS

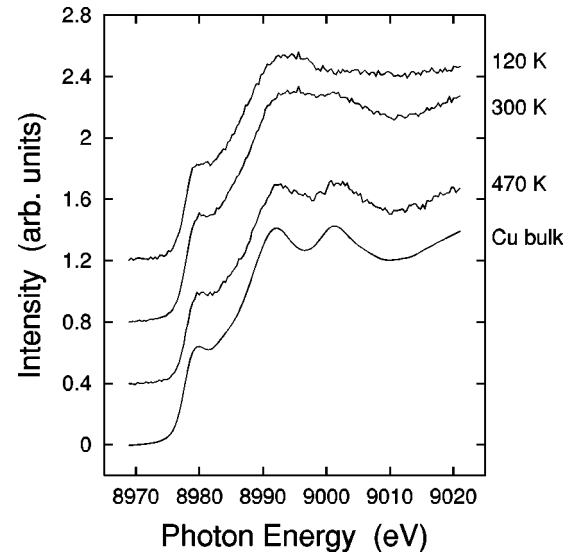


FIG. 1. Cu *K*-edge XANES spectra of the Cu 15-ML film prepared by the deposition at 120 K and annealing at 300 and 470 K, together with the spectrum of a Cu foil (bottom). The measurement temperatures are 120 K for the 15-ML film and 150 K for the Cu foil.

functions $\chi(k)$ (k is the photoelectron wave number) was carried out according to the well-established procedures:^{21,22} pre- and post-edge background subtractions and subsequent normalization with the atomic absorption coefficients. The edge energy ΔE_0 was tentatively chosen as an inflection point of the *K* edges in the 90° spectra. Figures 2 and 3 show, respectively, the $k^2\chi(k)$ functions and corresponding Fourier transforms for the Cu thin film after annealing at various temperatures, together with corresponding bulk ones. The k range employed in the Fourier transforms was $3.0\text{--}11.0 \text{ \AA}^{-1}$. In the Fourier transforms, the dominant peaks at 2.0 \AA are ascribed to the first-nearest-neighbor (NN) metal-metal coordination. A drastic change has appeared in the 120-K spectrum. A smaller EXAFS amplitude indicates

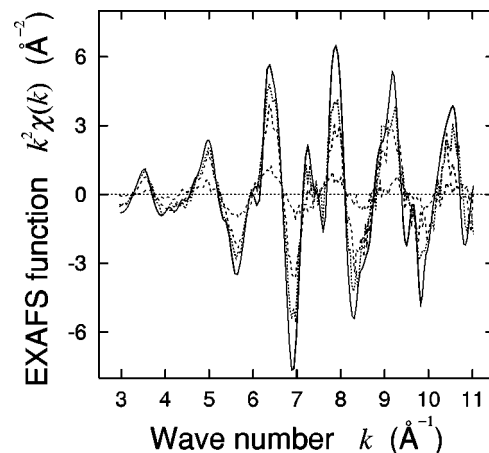
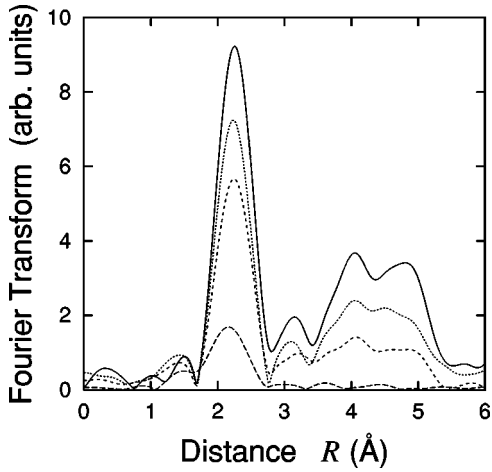


FIG. 2. Cu *K*-edge EXAFS oscillation functions $k^2\chi(k)$ of the Cu 15-ML film prepared by the deposition at 120 K (long-dashed line) and annealing at 300 K (short-dashed line) and 420 K (dotted line) taken at normal x-ray incidence, together with the spectrum of the Cu foil (solid line). The measurement temperatures are 120 K for the 15-ML film and 150 K for the Cu foil.

FIG. 3. Fourier transforms of $k^2\chi(k)$ of Fig. 2.

smaller coordination number and larger disorder of the film. The absence of higher shells means that the film does not crystallize completely.

The curve-fitting analysis of the first-NN shells was performed in k space after Fourier filtering ($\Delta R = 1.7\text{--}2.8$ Å) and inverse Fourier transformation. The backscattering amplitudes and phase shifts for the shells were obtained from the empirical references of bulk Cu. Fitting parameters employed were N^* (effective coordination number), R (interatomic distance), C_2 (mean-square relative displacement), and C_3 (mean-cubic relative displacement). The edge-energy shift ΔE_0 was assumed to be equal to those of the bulks. The numerical results are summarized in Table I. Although it might not be appropriate to analyze such a disorder system in a usual way, the estimated N^* was 4.7 ± 0.3 , which is much smaller than the bulk value of 12, and R was 2.52 ± 0.01 Å, which is also shorter than that of bulk Cu, 2.55 Å. The small N^* and R values are also observed for metal small clusters.^{8–13} The films can be regarded as an assembly of small clusters after deposition at low temperature. After annealing the film, N^* , R , C_2 , and C_3 converged to the bulk Cu value. We could qualitatively investigate the crystal growth process from the microscopic point of view. Considering the LEED results, it is revealed that the (111)-oriented large crystals (films) are formed by deposition at low temperature and subsequent annealing to room temperature.

B. Thermal vibration of Cu and Ni films

4-ML-thick Ni and 4- and 8-ML-thick Cu epitaxial films were prepared by deposition at low temperature and subsequent annealing to room temperature. Figures 4 and 5 show, respectively, the $k^2\chi(k)$ functions and corresponding Fourier

TABLE I. Structural parameters determined by EXAFS for the Cu 15-ML film. All the measurement temperatures are 120 K.

State	N	R (Å)	C_2 (10^{-3} Å ²)	C_3 (10^{-4} Å ³)
As deposited at 120 K	4.7(3)	2.52(1)	3.8(4)	5.5(7)
Annealed at 300 K	8.3(3)	2.55(1)	1.6(2)	2.3(4)
Annealed at 420 K	10.8(4)	2.55(1)	1.2(2)	2.0(4)

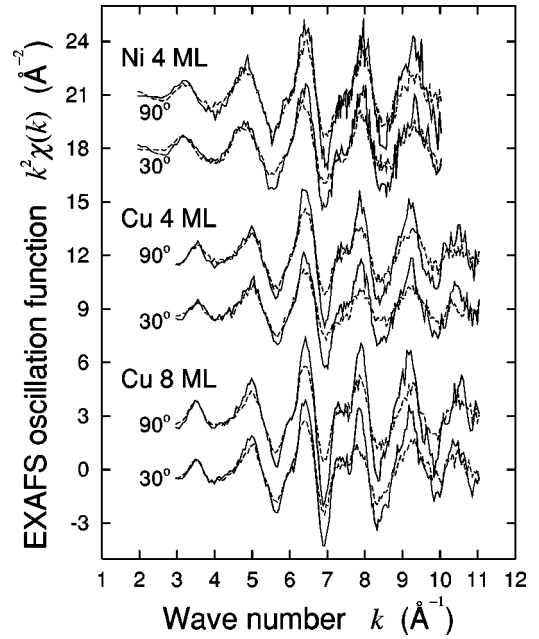


FIG. 4. Ni and Cu K -edge EXAFS oscillation functions $k^2\chi(k)$ of the Ni 4-ML and Cu 4- and 8-ML films measured at grazing (30°) and normal (90°) x-ray incidences at 120 K (solid line) and 300 K (dotted line).

transforms of them. The curve-fitting analysis of the first-NN shells in the 120-K data was subsequently performed in a similar manner ($\Delta k = 2\text{--}10$ Å⁻¹ and $\Delta R = 1.6\text{--}2.7$ Å for Ni) and the results are summarized in Table II. C_3 is neglected because of the low-temperature analysis of the well-ordered films.

First of all, we will discuss the effective coordination number N^* . N^* is defined as

$$N^* = 3 \sum_{j=1}^N \cos^2 \theta_j, \quad (1)$$

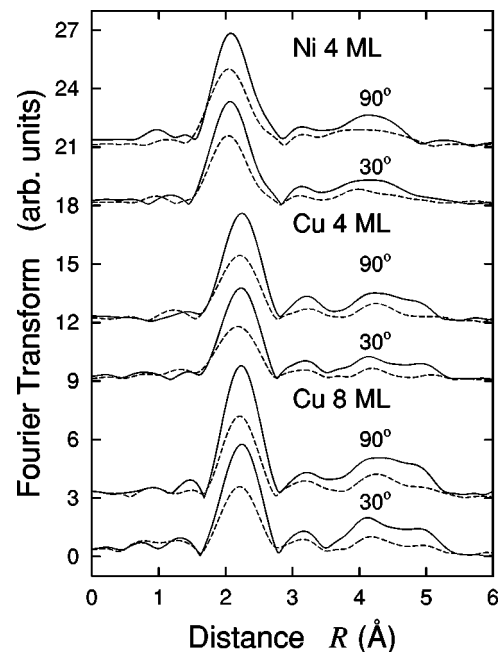


FIG. 5. Fourier transforms of $k^2\chi(k)$ of Fig. 4.

TABLE II. The EXAFS results for the first-NN metal-metal shells in the 4-ML Ni film and the 4- and 8-ML Cu films.

System	Angle	N	$R(\text{\AA})$	$C_2(10^{-3} \text{\AA}^2)$
Ni 4 ML	90°	9.2(7)	2.47(2)	5.8(3)
	30°	8.4(3)	2.47(1)	5.8(2)
Ni bulk		12	2.47	3.2
Cu 4 ML	90°	10.2(3)	2.54(1)	5.6(3)
	30°	8.6(3)	2.53(1)	5.8(3)
Cu 8 ML	90°	10.9(3)	2.54(1)	5.2(2)
	30°	10.4(4)	2.54(1)	5.8(3)
Cu bulk		12	2.55	4.0

where θ_j is the angle between \mathbf{E} and the location vector from the x-ray-absorbing atom to x-ray-scattering atom j . An ideal flat 4-ML-thick film oriented in the (111) direction would provide $N^*(90^\circ) = 11.3$ and $N^*(30^\circ) = 9.2$, respectively. We obtained $N^*(90^\circ) = 10.2 \pm 0.3$ and $N^*(30^\circ) = 8.6 \pm 0.3$ for the Cu 4-ML film, and $N^*(90^\circ) = 9.2 \pm 0.7$ and $N^*(30^\circ) = 8.4 \pm 0.3$ for Ni 4-ML film. Although the absolute value is a little smaller than the expected values, polarization dependence of N^* [$N^*(90^\circ) > N^*(30^\circ)$] means that the flat (111)-oriented films were formed on the HOPG. Slightly smaller N^* and larger C_2 of the films may suggest imperfect flatness due to island formation. Smaller N^* of the Ni film indicates more difficulty in the formation of films than Cu. This is reasonable, taking account of the mobilities of Cu and Ni at room temperature (Debye temperatures of 450 K for Ni and 343 K for Cu).

The temperature dependence of the EXAFS spectra for the first-NN shells was subsequently analyzed by means of the curve-fitting method. Figure 6 shows the filtered $k^2\chi(k)$ functions for the first-NN Ni-Ni and Cu-Cu shells. It is clear that with a temperature rise the EXAFS amplitude is reduced and the phase is gradually delayed at high k regions. These phenomena can easily be understood by the third-order cumulant expansion formula of EXAFS:

$$k\chi(k) = A_0(k) \exp(-2C_2k^2) \sin[2kR + \phi(k) - 4/3C_3k^3], \quad (2)$$

where $A_0(k)$ and $\phi(k)$ are the amplitude factor and the phase shift, both of which are less temperature dependent. Because of the enhancement of C_2 and C_3 with a temperature rise, the amplitude is suppressed and the phase is gradually delayed. In the present analysis, the low-temperature (120 K) data were used as references. The fitting variables were R , C_2 , and C_3 for Cu, while for Ni, C_3 was neglected because it was too small to obtain quantitatively. The qualities of the curve fitting are exemplified in Fig. 7.

The results are tabulated in Table III. In Table III, ΔC_2 and ΔC_3 imply the differences in C_2 and C_3 between 120 K and 300 K. Large positive ΔC_2 and ΔC_3 mean large thermal vibrations and anharmonicity. Larger ΔC_2 and ΔC_3 of the films indicate that the effective interatomic potential should be shallower and more anharmonic. The present results are consistent with the results of small clusters; that is, the contraction of the bond length and the enhancement of thermal vibration and anharmonicity were also observed in small clusters.

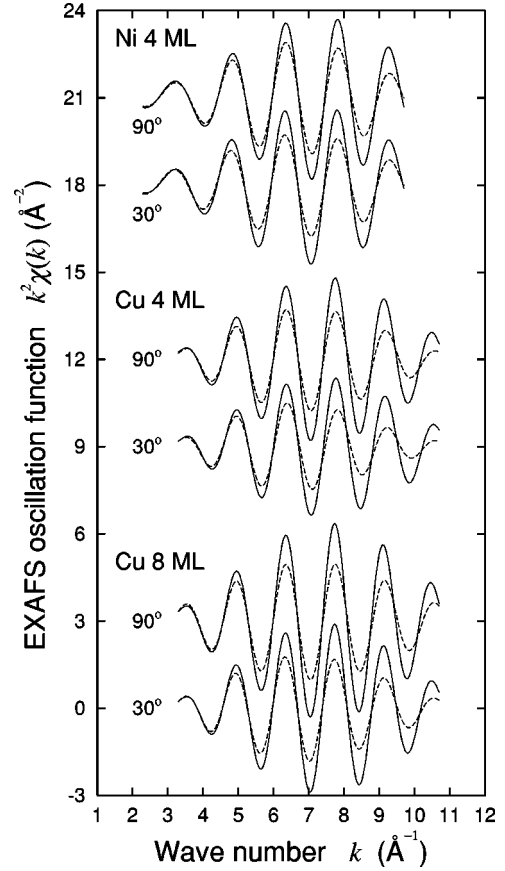


FIG. 6. Filtered EXAFS oscillation functions $k^2\chi(k)$ of the first-NN contributions at 120 (solid line) and 300 K (dotted line) for 30° and 90° x-ray incidences.

As concerns the polarization dependence, C_2 and C_3 show larger temperature dependence for $\theta = 30^\circ$ than for $\theta = 90^\circ$, indicating that the surface out-of-plane bond is softer and more anharmonic than the in-plane bond. The Debye temperature was estimated according to the well-known formula given by Beni and Platzman.²³ The Debye temperatures

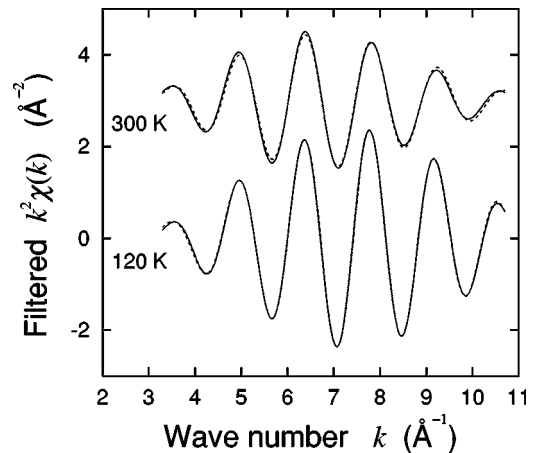


FIG. 7. Examples of the curve-fitting analysis for the first-NN Cu-Cu shells, which are obtained for the 4-ML Cu film measured at the x-ray incident angle of 30° at temperatures of 120 and 300 K. The filtered (experimental) and fitted (calculational) EXAFS oscillation functions $k^2\chi(k)$ are given as solid and dotted lines, respectively.

TABLE III. The results of the temperature-dependent EXAFS analysis for the first-NN metal-metal shells in the 4-ML Ni film and the 4 and 8-ML Cu films.

System	Angle	$\Delta C_2(10^{-3} \text{ \AA}^2)$	$\Delta C_3(10^{-4} \text{ \AA}^3)$	$\Theta_D(\text{K})$
Ni 4 ML	90°	3.4(4)		366(20)
	30°	4.0(4)		345(15)
Ni bulk		2.6		416
Cu 4 ML	90°	4.4(4)	3.1(6)	325(15)
	30°	5.0(5)	3.8(8)	307(15)
Cu 8 ML	90°	4.3(4)	2.3(4)	328(15)
	30°	4.4(4)	2.7(6)	325(15)
Cu bulk		4.0	1.4	338

for all the shells are also tabulated in Table III, together with the corresponding bulk value. Although there might be some difference between the cumulants for 30° and 90°, they are unfortunately within the errors.

Let us here argue from the statistical point of view whether the differences in the anisotropic vibration are significant. We employ the ratio of cumulants between 30° and 90°, for ΔC_2 , which are 1.18 ± 0.20 , 1.14 ± 0.15 , and 1.02 ± 0.14 for Ni (4 ML), Cu (4 ML), and Cu (8 ML), respectively, and for ΔC_3 which are 1.23 ± 0.42 and 1.18 ± 0.47 for Cu (4 ML) and Cu (8 ML), respectively. If the values are significantly greater than unity, the difference between the 30° and 90° data becomes meaningful. The probability density function of true values (τ) can be expressed with the normal Gaussian distribution with the average value (μ) of the measured value and the standard deviation (ρ) of its error. The probability P that the true value τ is located between $\mu - \rho$ and $\mu + \rho$ is given by $P(\mu - \rho < \tau < \mu + \rho) = 0.68$, and $P(\tau \leq 1) = 0.18$ is thus obtained when $\mu = 1.18$ and $\rho = 0.20$ for ΔC_2 of Ni (4 ML). Similarly, we obtain $P(\tau \leq 1) = 0.18$ and 0.44 for ΔC_2 of Cu (4 and 8 ML), and $P(\tau \leq 1) = 0.29$ and 0.35 for ΔC_3 of Cu (4 and 8 ML). Since each event is independent of each other, $P(\tau \leq 1)$ for all the cases is resultantly estimated to be 0.014 for ΔC_2 and 0.10 for ΔC_3 , assuming the perfect correlation among the three data sets of Ni (4 ML) and Cu (4 and 8 ML). Moreover, one may permit the correlation between ΔC_2 and ΔC_3 because in a normal interatomic potential anharmonicity is enhanced with the suppression of the harmonic force constant. One can thus estimate the overall $P(\tau \leq 1)$ of 0.0014. We can conclude with the accuracy of 99.86% that the out-of-planar vibration for the surface metal-metal bonds is softer and/or more anharmonic than the in-planar one.

IV. MONTE CARLO SIMULATIONS

Classical N - P - T (closed system, constant pressure, and constant temperature) MC calculations of five-layer Cu were carried out in order to understand the surface vibration more deeply. Desjonquères and Trégliá have already calculated MSRD for various bulk metals and corresponding surfaces for a similar purpose.²⁴ They used a lattice dynamical model involving central forces between the first- and second-nearest neighbors and also bending interaction between triplets of first neighbors within the harmonic approximation. For the

description of the thermal properties of metals, however, these approximations might sometimes not be sufficient since the metallic bond should be of many body and the anharmonic effect is important. It is worthwhile performing MC simulations to compare the results with our present experiments and their lattice dynamics calculations.

For the description of the interatomic potential, the EAM was employed. In the EAM, the total adiabatic potential energy of the system can be written as a sum of short-range pairwise core-core repulsion and embedding energy for placing an atom into the electron density.^{25–28} The EAM does not require the three-dimensional periodicity and is thus applicable to surfaces as well as alloys and defects. The EAM parameters employed in the present simulations were determined by Foiles *et al.*²⁸

Five-layer Cu was taken into account in the N - P - T MC simulations. Here, a two-dimensional periodic boundary condition was imposed for a $12a \times 7\sqrt{6}a = 30.6 \times 30.917 \text{ \AA}^2$ rectangular lattice, where a is the interatomic Cu-Cu distance of 2.55 Å. Each Cu layer contains 168 atoms, and the lowest (fifth) layer was dynamically fixed at the bulk position, although the lattice constant was allowed to vary. The MC calculations were based on the Metropolis algorithms. Initially, 20 000 MC steps were evaluated from the ideal bulk lattice, where each step contains 672 times movements of atoms and one time variation of the lattice constant. After the 20 000 MC steps, 10 000 MC steps were further calculated to get information on thermodynamical averages. The external pressure P was assumed to be 0 Pa, and the temperatures were set to be 120 and 300 K.

The second- and third-order cumulants C_2 and C_3 given by the present EAM-MC calculations are summarized in Table IV. Here, Cu1, Cu2, and Cu3 denote the Cu atoms in the first, second, and third layers, respectively. Cu1-Cu1 means the in-plane bond in the first layer, while Cu1-Cu2 is the out-of-plane bond between the first and the second layer. For comparison, the experimental and previous calculation results of bulk Cu (Ref. 29) are also tabulated. We included the results of quantum-mechanical calculations and those of the classical calculations. For a quantitative comparison of the present classical MC results with the experimental ones, the contribution of zero point vibrations is required, thus indicating a slight underestimation of C_2 especially at low temperature and thus overestimation of ΔC_2 between 120 and 300 K.

As given in Table IV, the values of C_2 and C_3 of in-plane bonds like Cu1-Cu1 are large at the surface and decrease as they go into the bulk and converge to the bulk value at the third layer. Such increases in thermal vibrations of in-plane bonds are consistent with large ΔC_2 and ΔC_3 observed experimentally in the normal incidence spectra. As concerns the anisotropy of the thermal vibrations of the Cu-Cu bonds, C_2 of the out-of-plane bonds (Cu1-Cu2) is larger than that of in-plane bonds (Cu1-Cu1 and Cu2-Cu2). This agrees with the experimental results whereby the bonds observed experimentally at grazing incidence are softer and more anharmonic than the ones at normal incidence. We could reproduce the experimental results qualitatively, and show that the bonds between the first and second layers are especially soft.

The lattice dynamic calculations by Desjonquères and Trégliá²⁴ have demonstrated that C_2 of the out-of-plane bond

TABLE IV. Cumulants for the Cu-Cu shell in Cu 4-ML film at 120 and 300 K estimated from the MC simulations. The experimental and calculated values for bulk Cu are also given for comparison. All the quantities of C_2 are in units of 10^{-3} \AA^2 and those of C_3 are in 10^{-4} \AA^3 .

	ΔC_2	C_2 (120 K)	C_2 (300 K)	ΔC_3	C_3 (120 K)	C_3 (300 K)
4-ML Cu films						
Classical MC						
Cu1-Cu1	5.64	3.47	9.11	2.12	0.34	2.46
Cu2-Cu2	5.43	3.23	8.66	1.99	0.17	2.16
Cu3-Cu3	5.00	2.94	7.94	0.88	0.22	1.10
Cu1-Cu2	5.94	3.67	9.61	2.15	0.47	2.62
Cu2-Cu3	5.33	3.13	8.46	1.71	0.17	1.88
Experimental						
90°	4.4(4)			3.1(6)		
30°	5.0(5)			3.8(8)		
fcc Cu bulk (Ref. 29)						
Classical	5.14	3.21	8.35	1.48	0.26	1.74
Quantum	4.61	4.19	8.80	1.48	0.26	1.74
Experimental	4.03	4.00	8.03	1.4		

is not very sensitive to the nature of the metal or to the crystallographic orientation of the surface. They found the relation as $C_2(\text{Cu1-Cu2}) \sim 1.14 \times C_2(\text{bulk Cu-Cu})$. In contrast, C_2 of the in-plane bond is much closer to the bulk value although it depends on metals. They obtained the relation like $C_2(\text{Cu1-Cu1}) \sim 1.03 \times C_2(\text{bulk Cu-Cu})$ for Cu(111). On the other hand, our classical MC results were $\Delta C_2(\text{Cu1-Cu2}) = 1.16 \times \Delta C_2(\text{bulk Cu-Cu})$ and $\Delta C_2(\text{Cu1-Cu1}) = 1.10 \times \Delta C_2(\text{bulk Cu-Cu})$. Note here that the value of $\Delta C_2(\text{bulk Cu-Cu})$ used is the classical one to match the present MC calculations. The present results agree with the experiments and the previous lattice dynamics calculations²⁴ at least qualitatively. Although we obtained more enhanced surface vibrations than those by Desjonquères and Tréglià, we can conclude that thermal vibrations of the out-of-plane bonds are more enhanced than those of the in-plane ones. The quantitative differences might originate from the differences of models, potentials, or quantum effects.

V. DISCUSSION

Although the vibrational anisotropy has been studied for various kinds of adsorbate-substrate systems,^{14,30-32} no unified conclusions have been obtained. As mentioned in Sec. I, Roubin *et al.*¹⁴ have showed that in the Co/Cu(111) system the surface out-of-plane (Co-Cu) bond is softer than the in-plane (Co-Co) one. On the contrary, Wenzel *et al.*^{30,31} have revealed that in the N/Ni(100)-*p*4g(2×2) system, the in-plane N-Ni bond is softer than the out-of-plane one. More recently, Yokoyama *et al.*³² have studied systematically the thermal vibrations of the first- and second-NN bonds for S/Ni(100)-*c*(2×2) and S/Ni(110)-*c*(2×2). They have suggested a simple argument that the longer bond simply provides softer and more anharmonic vibrations than the shorter ones; in S/Ni(100), the first-NN S-Ni bond ($R_1 = 2.19 \text{ \AA}$) directed in the in-plane direction is stiffer than the out-of-plane second-NN one ($R_2 = 3.12 \text{ \AA}$), while in S/Ni(110) the

first-NN out-of-plane bond ($R_1 = 2.19 \text{ \AA}$) is stiffer than the in-plane second-NN nearest bond ($R_2 = 2.27 \text{ \AA}$). Although this simple concept can explain the above vibrational anisotropy of Co/Cu(111) and N/Ni(100) systems, it is not clear whether the in-plane and out-of-plane bonds show the same vibrational properties if their bond distances are equivalent. In this paper, we have studied anisotropic vibrational properties of ultrathin films, and have revealed that the out-of-plane bond is softer than the in-plane bond even if the bond distance is not different.

Let us here estimate the vibrational amplitudes of the in-plane and out-of-plane bonds quantitatively using the present EXAFS results. We can suppose that only the in-plane bond in the first layer and the bond between the first and second layers show different vibrational amplitudes from the bulk ones, while all the other bonds are of bulk Cu. This assumption is based on the above MC results; the thermal vibrations of Cu1-Cu1 and Cu1-Cu2 are different from those of bulk ones. Let us define C_2^{si} , C_2^{so} , and C_2^{b} as the MSRD of Cu1-Cu1, Cu1-Cu2, and the other Cu-Cu bonds, respectively. The C_2 value observed experimentally can be given as

$$C_2(m, \theta) = \frac{(C_2^{\text{so}} + 6C_2^{\text{si}})\sin^2\theta + 4C_2^{\text{so}}\cos^2\theta + 4C_2^{\text{b}}(m-2)}{4m - 4 + 3\sin^2\theta}, \quad (3)$$

where m and θ are the film thickness and x-ray incidence angle, respectively. By using experimental results of ΔC_2 given in Table III, we can obtain each component as $\Delta C_2^{\text{so}} = (7.0 \pm 1.4) \times 10^{-3} \text{ \AA}^2$, $\Delta C_2^{\text{si}} = (4.5 \pm 0.9) \times 10^{-3} \text{ \AA}^2$, and $\Delta C_2^{\text{b}} = (4.1 \pm 0.4) \times 10^{-3} \text{ \AA}^2$. The corresponding Debye temperatures are $\Theta_{\text{D}}^{\text{so}} = 262(25) \text{ K}$, $\Theta_{\text{D}}^{\text{si}} = 322(30) \text{ K}$, and $\Theta_{\text{D}}^{\text{b}} = 335(5) \text{ K}$, respectively, which are depicted in Fig. 8. The Debye temperature of bulk Cu is 343 K by calorimetric measurements,³³ and 338 K by EXAFS. Our present result of $\Theta_{\text{D}}^{\text{b}} = 335(5) \text{ K}$ indicates high reliability of the present model.

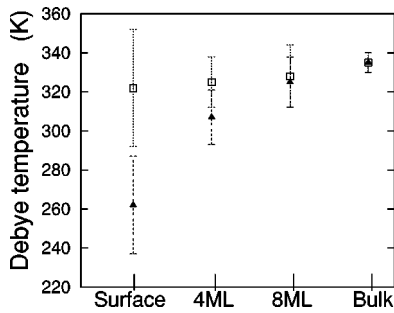


FIG. 8. Effective Debye temperature of the surface Cu atoms, 4- and 8-ML Cu films, and bulk Cu. The out-of-plane and in-plane ones are given as closed triangles and open squares, respectively. See the text for details.

Moreover, we can estimate the relations as $\Delta C_2^{\text{so}} = 1.71 \times \Delta C_2^{\text{b}}$ and $\Delta C_2^{\text{si}} = 1.10 \times \Delta C_2^{\text{b}}$. The lattice dynamics calculations²⁴ gave $\Delta C_2^{\text{so}} = 1.14 \times \Delta C_2^{\text{b}}$ and $\Delta C_2^{\text{si}} = 1.03 \times \Delta C_2^{\text{b}}$, while our MC results gave $\Delta C_2^{\text{so}} = 1.16 \times \Delta C_2^{\text{b}}$ and $\Delta C_2^{\text{si}} = 1.10 \times \Delta C_2^{\text{b}}$. These two calculations seem to underestimate the surface vibrations and anisotropy compared to the present experimental results. Note here that the surface Debye temperature of Cu(100) determined by LEED is 235 K,³ which is still lower than the present result of 262 K. We can suppose that the reason for larger ΔC_2 and ΔC_3 observed experimentally is that theoretical calculations treat perfect films, while the actual films contain many defects and some roughening might occur already at room temperature, as is evident from smaller N^* and larger C_2 . Since the surface area becomes wider in the presence of defects, the surface Debye temperature would effectively be lowered.

We can further compare the present results with those of ultrafine particles. The thermal vibrations of metal surfaces have been studied for small metal clusters.⁸⁻¹³ The increase in the thermal vibration and anharmonicity have been observed with a decrease in cluster size. The decrease in the Debye temperature is caused by softening of the metal-metal

vibrational frequencies. Harada and Ohshima¹² have studied the mean-square displacements for Au small clusters as a function of a cluster size by using x-ray diffraction. They also assumed that the particle is composed of the core and shell. They have shown that when the thickness of the shell is assumed as one atomic layer, $\Theta_{\text{D}}(\text{core}) = 165$ K and $\Theta_{\text{D}}(\text{shell}) = 97$ K are in good agreement with the reported values of $\Theta_{\text{D}}(\text{bulk}) = 168$ K and $\Theta_{\text{D}}(\text{shell}) = 83$ K, the latter of which was determined by LEED.

VI. CONCLUSION

Angular- and temperature-dependent Cu and Ni *K*-edge EXAFS spectra of 4 and 8 ML Cu and 4 ML Ni grown epitaxially on HOPG have been measured and analyzed in order to investigate the dynamical properties of the surface metal-metal bonds. It was revealed that thermal vibration and local thermal expansion of the metal-metal bond are larger for the films than for their corresponding bulk metals and the relative motions focused on the surface local bonds are enhanced in the surface normal direction. In the present study, by changing x-ray incidence angle and film thickness, we could separate the thermal vibrations of the surface in-plane and out-of-plane and bulk bonds, and discuss the bond character quantitatively. For further understanding of thermal vibrations, we have done classical Monte Carlo calculations for the Cu film and revealed that the out-of-plane bond between the first and second layer is very weak.

ACKNOWLEDGMENTS

The present work has been performed under the approval of Photon Factory Program Advisory Committee (PF-PAC No. 98G101 and 98G314). The authors gratefully acknowledge Professor Masaharu Nomura and Atsushi Koyama for their technical support for the XAFS measurements. The authors are also grateful for the financial support of the Grant-in-Aid for Scientific Research (No. 09640598).

- ¹A.U. MacRae, *Surf. Sci.* **2**, 52 (1964).
- ²Y. Cao and E. Conrad, *Phys. Rev. Lett.* **65**, 2808 (1990).
- ³S. Müller, A. Kinne, M. Kottke, R. Metzler, P. Bayer, L. Hammer, and K. Heinz, *Phys. Rev. Lett.* **75**, 2859 (1995).
- ⁴K. Pohl, J.H. Cho, K. Terakura, M. Scheffler, and E.W. Plummer, *Phys. Rev. Lett.* **80**, 2853 (1998).
- ⁵A.W. Denier van der Gon, R.J. Smith, J.M. Gay, D.J. O'connor, and J.F. van der Veen, *Surf. Sci.* **227**, 143 (1990).
- ⁶J.W.M. Frenken and J.F. van der Veen, *Phys. Rev. Lett.* **54**, 134 (1985).
- ⁷E.A. Stern, P. Liviš, and Z. Zhang, *Phys. Rev. B* **43**, 8850 (1991).
- ⁸A. Balerna, E. Bernieri, P. Picozzi, A. Reale, S. Santucci, E. Burattini, and S. Mobilio, *Phys. Rev. B* **31**, 5058 (1985).
- ⁹P.A. Montano, G.K. Shenoy, E.E. Alp, W. Schulze, and J. Urban, *Phys. Rev. Lett.* **56**, 2076 (1986).
- ¹⁰G. Apai, J.F. Hamilton, J. Stöhr, and A. Thompson, *Phys. Rev. Lett.* **43**, 165 (1979).
- ¹¹T. Yokoyama, S. Kimoto, and T. Ohta, *Jpn. J. Appl. Phys., Part 2* **28**, L851 (1989).
- ¹²J. Harada and K. Ohshima, *Surf. Sci.* **106**, 51 (1981).
- ¹³P. Buffat and J. Borel, *Phys. Rev. A* **13**, 2287 (1976).
- ¹⁴P. Roubin, D. Chandèsris, G. Rossi, J. Lecante, M.C. Desjonquères, and G. Tréglia, *Phys. Rev. Lett.* **56**, 1272 (1986).
- ¹⁵F. Patthey and W.D. Schneider, *Phys. Rev. B* **50**, 17 560 (1994).
- ¹⁶F. Patthey and W.D. Schneider, *Surf. Sci.* **334**, L715 (1995).
- ¹⁷G. Neuhold and K. Horn, *Phys. Rev. Lett.* **78**, 1327 (1997).
- ¹⁸M. Bäumer, J. Libuda, and H.J. Freund, *Surf. Sci.* **327**, 321 (1995).
- ¹⁹P. Marcus and C. Hinnen, *Surf. Sci.* **392**, 134 (1997).
- ²⁰M. Nomura and A. Koyama, in *X-Ray Absorption Fine Structure*, edited by S. S. Hasnain (Ellis Horwood, Chichester, 1991), p. 667.
- ²¹See, for instance, *X-ray Absorption: Principles, Applications, Techniques of EXAFS, SEXAFS and XANES*, edited by D.C. Koningsberger and R. Prins (Wiley, New York, 1988).
- ²²T. Yokoyama, H. Hamamatsu, and T. Ohta, EXAFSH, version 2.1 (The University of Tokyo, Tokyo, 1993).

- ²³G. Beni and P.M. Platzman, Phys. Rev. B **14**, 1514 (1976).
- ²⁴M.C. Desjonquères and G. Tréglia, Phys. Rev. B **34**, 6662 (1986).
- ²⁵M.S. Daw and M.I. Baskes, Phys. Rev. B **29**, 6443 (1984).
- ²⁶S.M. Foiles, Phys. Rev. B **32**, 3409 (1985).
- ²⁷S.M. Foiles, Phys. Rev. B **32**, 7685 (1985).
- ²⁸S.M. Foiles, M.I. Baskes, and M.S. Daw, Phys. Rev. B **33**, 7983 (1986).
- ²⁹T. Yokoyama, Phys. Rev. B **57**, 3423 (1998).
- ³⁰L. Wenzel, J. Stöhr, D. Arvanitis, and K. Baberschke, Phys. Rev. Lett. **60**, 2327 (1988).
- ³¹L. Wenzel, D. Arvanitis, H. Rabus, T. Lederer, K. Baberschke, and G. Comelli, Phys. Rev. Lett. **64**, 1765 (1990).
- ³²T. Yokoyama, H. Hamamatsu, Y. Kitajima, Y. Takata, S. Yagi, and T. Ohta, Surf. Sci. **313**, 197 (1994).
- ³³C. Kittel, *Introduction to Solid State Physics* (Wiley, New York, 1988).